

# Stability of neural ODEs by a control over the expansivity of their flows

Arturo De Marinis<sup>\*1</sup>, Nicola Guglielmi<sup>†1</sup>, Stefano Sicilia<sup>‡1</sup>, and Francesco Tudisco<sup>§1,2</sup>

<sup>1</sup>Gran Sasso Science Institute, L'Aquila, Italy

<sup>2</sup>The University of Edinburgh, Edinburgh, United Kingdom

## Abstract

We propose a method to enhance the stability of a neural ordinary differential equation (neural ODE) by means of a control over the Lipschitz constant  $C$  of its flow. Since it is known that  $C$  depends on the logarithmic norm of the Jacobian matrix associated with the neural ODE, we tune this parameter at our convenience by suitably perturbing the Jacobian matrix with a perturbation as small as possible in Frobenius norm. We do so by introducing an optimization problem for which we propose a nested two-level algorithm. For a given perturbation size, the inner level computes the optimal perturbation with a fixed Frobenius norm, while the outer level tunes the perturbation amplitude. We embed the proposed algorithm in the training of the neural ODE to improve its stability. Numerical experiments on the MNIST and FashionMNIST datasets show that an image classifier including a neural ODE in its architecture trained according to our strategy is more stable than the same classifier trained in the classical way, and therefore, it is more robust and less vulnerable to adversarial attacks.

## 1 Introduction

A neural ODE [1] is an ordinary differential equation of the form

$$\dot{x}(t) := \frac{d}{dt}x(t) = \sigma(Ax(t) + b), \quad t \in [0, T], \quad (1)$$

where the state  $x(t) \in \mathbb{R}^n$  is a feature vector,  $\sigma : \mathbb{R} \rightarrow \mathbb{R}$  is a smooth activation function applied entry-wise,  $T > 0$  is the time horizon,  $A \in \mathbb{R}^{n,n}$  is the weight matrix and  $b \in \mathbb{R}^n$  is the bias vector.

The discretization of (1) determines a special kind of deep neural network, denoted as residual neural network (ResNet). Given a partitioning  $0 = t_0 < t_1 < \dots < t_N = T$  of the interval  $[0, T]$ , the Euler method applied to (1) yields indeed the residual neural network [2]

$$x_{k+1} = x_k + h\sigma(Ax_k + b), \quad k = 0, 1, \dots, N-1,$$

with  $x_k \approx x(t_k)$  and  $h = T/N$ .

<sup>\*</sup>arturo.demarinis@gssi.it

<sup>†</sup>nicola.guglielmi@gssi.it

<sup>‡</sup>stefano.sicilia@gssi.it

<sup>§</sup>f.tudisco@ed.ac.uk

The advantage of defining a neural network from a differential equation consists in the possibility of studying its properties starting from those of the ODE. In particular, contractivity, stability and conservation properties, see e.g. [3].

The goal of this article is to design deep neural networks robust against adversarial attacks [4, 5, 6], i.e. perturbations in the input data with the scope to make a neural network return a wrong output. Under suitable Lipschitz assumptions on the vector field, the neural ODE (1) satisfies the following condition: there exists a constant  $C > 0$  such that, for any two solutions  $x_1(t)$  and  $x_2(t)$  originating from initial data  $x_1(0) \neq x_2(0)$ , it holds

$$\|x_1(t) - x_2(t)\| \leq C\|x_1(0) - x_2(0)\|, \quad t \in [0, T], \quad (2)$$

where  $\|\cdot\|$  denotes a certain norm in  $\mathbb{R}^n$ . This means that, depending on the constant  $C$ , the neural ODE shows different behaviours. In particular, the neural ODE is contractive if  $C < 1$ . We could say that a stable neural ODE is characterized by a constant  $C$  of moderate size. In contrast, if  $C \gg 1$ , small perturbations in the input may cause large changes in the output.

Under the assumption that the numerical discretization of (1) preserves the stability/contractivity properties of the exact solution [7], we can construct a deep residual network that is either stable/contractive, making it robust against adversarial attacks. However, asking for a contractive or strongly stable property may result in a loss of accuracy of the neural network. For instance, in a classification problem, the percentage of correctly classified test data could decrease significantly when contractivity is imposed. This trade-off is unavoidable, as well as it has been shown, viceversa, that an overly accurate neural network will eventually become unstable [8]. Consequently, there is a compromise to reach when optimizing for both accuracy and robustness, which means that a constant  $C > 1$  of moderate size would be an acceptable choice. Building on this idea, we propose a two-level optimization strategy, enabling us to optimize the weight matrix  $A$  and the vector  $b$ , controlling on the one side the accuracy of the neural network and on the other side the Lipschitz constant  $C$ .

Our approach involves computing the closest perturbation (possibly structured) of the weight matrix  $A$  that allows to obtain the desired constant  $C$  as a stability bound. We demonstrate the effectiveness of this strategy by means of few numerical experiments on standard classification benchmarks.

## 1.1 Paper organization

The paper is organized as follows. In Section 2 the stability of neural ODEs is studied from a theoretical point of view; contractivity in the 2-norm is recalled and adapted to the considered problem. Next, a two-level algorithm is proposed, with the aim of modifying the matrix  $A$  in order to reach the stability goal for the solution of the neural ODE. The two-level approach taken here uses an *inner iteration* to compute the solution of a suitable eigenvalue optimization problem associated to the required stability property (which requires the uniform control of the logarithmic norm of the matrix  $A$  premultiplied by a diagonal matrix) for a fixed perturbation size  $\varepsilon$  of the allowed perturbations of  $A$ , and then determines the optimal perturbation size  $\varepsilon$  in an *outer iteration*, that is the perturbation of minimal size that allows to obtain the desired stability bound.

Section 3 describes the inner iteration of the two-level algorithm, and Section 4 discusses the solution of the outer iteration. Section 5 shows how the proposed algorithm is embedded in the training of the neural ODE to improve its stability and robustness to adversarial attacks. Numerical experiments on MNIST and FashionMNIST datasets classification are reported. Finally, Section 6 draws our conclusions.

## 1.2 Existing literature on the stability of neural ODEs

Many papers have explored the idea of interpreting and studying deep residual neural networks as discretizations of continuous-time ordinary differential equations (ODEs). Early works in this direction include [1, 9, 10, 11], with Chen et al. [1] popularizing the term *Neural Ordinary Differential Equation*. As noted already in [9], tools from the stability theory of ODEs can be highly effective for analysing and enhancing the adversarial robustness of residual networks modelled as discretizations of continuous-time neural ODEs. Since then, the literature on this topic has expanded significantly, with many recent works focusing on the stability properties of neural ODEs.

Carrara et al. [12] analyse the robustness of image classifiers implemented as neural ODEs against adversarial attacks and compare their performance to standard deep models. They empirically demonstrate that neural ODEs are inherently more robust to adversarial attacks than state-of-the-art residual networks. Yan et al. [13] reach similar conclusions. They offer a deeper understanding of this phenomenon by leveraging a desirable property of the flow of a continuous-time ODE: integral curves are non-intersecting. For three initial points, the integral curve starting from the middle point is always sandwiched between the integral curves starting from the others. This imposes a bound on the deviation from the original output caused by a perturbation in the input. In contrast, state-of-the-art residual networks lack such bounds on output deviation, making neural ODEs intrinsically more robust.

Li et al. [14] investigate the vulnerability of neural networks to adversarial attacks from the perspective of dynamical systems. By interpreting a residual network as an explicit Euler discretization of an ordinary differential equation, they observe that the adversarial robustness of a residual network is linked to the numerical stability of the corresponding dynamical system. Specifically, more stable numerical schemes may lead to more robust deep networks. Since implicit methods are more stable than explicit ones, they propose using the implicit Euler method instead of the explicit one to discretize the neural ODE, resulting in a more robust model.

Carrara et al. [15, 16] and Caldelli et al. [17] demonstrate that adversarial robustness can be enhanced by operating the network in different tolerance regimes during training and testing. Notably, robustness is further improved when the test-time tolerance is greater than the training-time tolerance, which is typically the same value used by the adversarial attacker.

Kang et al. [18] and Li et al. [19] propose a Stable neural ODE with Lyapunov-stable equilibrium points for Defending against adversarial attacks (SODEF). By ensuring that the equilibrium points of the ODE are Lyapunov-stable, and by minimizing the maximum cosine similarity between them, the solution for an input with a small perturbation converges to the same solution as the unperturbed initial input.

Huang et al. [20] introduce a provably stable architecture for neural ODEs that achieves non-trivial adversarial robustness even when trained without adversarial examples. Drawing inspiration from dynamical systems theory, they design a stabilized neural network whose neural ODE blocks are not symmetric, proving it to be input-output stable.

Cui et al. [21] propose a novel activation function called half-Swish and demonstrate that neural ODEs with this activation outperform those with standard activation functions in terms of robustness against adversarial attacks.

Purohit [22] advocates for the use of orthogonal convolutional layers to define the neural network dynamics of the ODE. This approach ensures that the representations of clean samples and their adversarial counterparts remain close, enhancing model robustness.

Ruthotto et al. [9, 11], Celledoni et al. [23], and Sherry et al. [24] explore a specific class of structured neural ODEs that are inherently non-expansive, making them robust to adversarial attacks by construction.

## 2 Stability of neural ODEs

As in Kang et al. [18] and Li et al. [19], our goal is to make a neural ODE stable. We start with a one-layer weight-tied neural ODE

$$\dot{x}(t) = \sigma(Ax(t) + b), \quad t \in [0, T], \quad (3)$$

where  $x(t) \in \mathbb{R}^n$  is the feature vector evolution function,  $A \in \mathbb{R}^{n,n}$  and  $b \in \mathbb{R}^n$  are the parameters, and  $\sigma : \mathbb{R} \rightarrow \mathbb{R}$  is a smooth activation function applied entry-wise. Later, we will provide details on how to extend to the two-layer weight-tied neural ODE

$$\dot{x}(t) = \sigma(A_2\sigma(A_1x(t) + b_1) + b_2), \quad t \in [0, T],$$

which then directly transfer to the general multi-layer case.

We require that  $\sigma'(\mathbb{R}) \subset [m, 1]$ , where  $0 < m \leq 1$  is a parameter. For most activation functions,  $\sigma'(\mathbb{R}) \subset [0, 1]$ , but in our setting we need  $\sigma'(x) \geq m > 0$ , for all  $x \in \mathbb{R}$ . This is easily achievable by means of a slight modification of the activation function without affecting the approximation capabilities of the neural ODE.

We wish, for any two solutions  $x_1(t)$  and  $x_2(t)$ , that the bound

$$\|x_1(t) - x_2(t)\|_2 \leq C\|x_1(0) - x_2(0)\|_2, \quad t \in [0, T],$$

is satisfied for a moderately sized constant  $C > 0$ , i.e. the stability condition (2). By denoting  $\langle \cdot, \cdot \rangle_2$  the standard inner product and  $f(t, x) = \sigma(Ax + b)$ , the stability condition above is satisfied if the one-sided Lipschitz condition holds

$$\langle f(t, x) - f(t, y), x - y \rangle_2 \leq \delta \|x - y\|_2^2, \quad t \in [0, T], \quad x, y \in \mathbb{R}^n, \quad (4)$$

for a certain  $\delta \in \mathbb{R}$ , which implies  $C = e^{\delta T}$ .

In our setting, we characterize the constants  $\delta$  and  $C$  by means of the logarithmic norm of the Jacobian of the activation function. In particular we consider the logarithmic 2-norm of a matrix  $M \in \mathbb{R}^{n,n}$ , that is defined as

$$\mu_2(M) = \lambda_{\max}(\text{Sym}(M)) := \max_{i=1, \dots, n} \lambda_i(\text{Sym}(M)), \quad (5)$$

where  $\lambda_i(\text{Sym}(M))$  denotes the  $i$ -th eigenvalue of the symmetric part of  $M$ .

Then, the one-sided Lipschitz condition (4) becomes

$$\begin{aligned} \langle \sigma(Ax + b) - \sigma(Ay + b), x - y \rangle_2 &= \langle J(x - y), x - y \rangle_2 = (x - y)^\top J(x - y) \\ &= (x - y)^\top \text{Sym}(J)(x - y), \end{aligned}$$

where  $J$  is the Jacobian matrix of  $\sigma(A \cdot + b)$  evaluated at  $\xi_\star$ ,

$$J = \left. \frac{d}{dx} \sigma(Ax + b) \right|_{x=\xi_\star} \in \mathbb{R}^{n,n},$$

where  $\xi_\star = (1 - t_\star)x + t_\star y$  for some  $t_\star \in [0, 1]$ , as provided by the mean value theorem. Note that, defined  $\mathbb{D}^{n,n}$  as the set of diagonal matrices of size  $n$  and

$$\Omega_m = \{D \in \mathbb{D}^{n,n} : m \leq D_{ii} \leq 1, \forall i = 1, \dots, n\},$$

the Jacobian  $J$  takes the form

$$J = \text{diag}(d)A := DA,$$

where  $d = \sigma'(A\xi_* + b)$  and  $\text{diag}(d)$  is the diagonal matrix whose diagonal is the vector  $d$ . Furthermore, note that writing  $x - y$  in terms of  $u_1, \dots, u_n \in \mathbb{R}^n$ , the orthonormal eigenvectors of  $\text{Sym}(J)$ ,

$$x - y = \sum_{i=1}^n \alpha_i u_i, \quad \alpha_i \in \mathbb{R},$$

yields

$$\begin{aligned} (x - y)^\top \text{Sym}(J)(x - y) &= \sum_{i=1}^n \alpha_i u_i^\top \sum_{j=1}^n \alpha_j \text{Sym}(J) u_j = \sum_{i=1}^n \lambda_i(\text{Sym}(J)) \alpha_i^2 \\ &\leq \left( \max_{i=1, \dots, n} \lambda_i(\text{Sym}(J)) \right) \sum_{i=1}^n \alpha_i^2 = \mu_2(J) \|x - y\|_2^2. \end{aligned}$$

By combining all together, we get

$$\langle \sigma(Ax + b) - \sigma(Ay + b), x - y \rangle_2 \leq \mu_2(J) \|x - y\|_2^2 \leq \max_{D \in \Omega_m} \mu_2(DA) \|x - y\|_2^2 := \delta \|x - y\|_2^2,$$

i.e. the neural ODE (3) satisfies the one-sided Lipschitz condition (4) with

$$\delta := \max_{D \in \Omega_m} \mu_2(DA) \quad (6)$$

and thus the stability condition (2) with  $C = e^{\delta T}$ . According to the sign of  $\delta$ , we get stability ( $\delta > 0$  small), nonexpansivity ( $\delta = 0$ ) and contractivity ( $\delta < 0$ ).

In light of (6) and the final remarks following (2), we would like the weight matrix  $A$  to be such that  $\delta$  is a positive constant of moderate size, so that the neural ODE (3) does not significantly amplify the perturbation in input. Since this fact generally does not happen if the neural ODE is trained using standard gradient methods, we impose it by computing the closest matrix  $B$  to  $A$  in a certain metric such that  $\mu_2(DB) = \delta$ , for all  $D \in \Omega_m$ . More precisely, we compute a matrix of the type

$$A_\delta \in A + \underset{\Delta \in \mathbb{R}^{n,n}}{\text{argmin}} \left\{ \|\Delta\|_F : \max_{D \in \Omega_m} \mu_2(D(A + \Delta)) = \delta \right\}, \quad (7)$$

where the Frobenius inner product of two matrices  $M, N \in \mathbb{R}^{n,n}$  and the corresponding Frobenius norm are defined as

$$\langle M, N \rangle_F = \text{tr}(N^\top M) = \sum_{i,j=1}^n M_{ij} N_{ij}, \quad \|M\|_F = \sqrt{\langle M, M \rangle_F}.$$

In this framework, it could be desirable that the perturbation  $\Delta$  has a certain structure, i.e.  $\Delta \in \mathcal{S}$ , where  $\mathcal{S}$  is a subspace of  $\mathbb{R}^{n,n}$ , for instance the space of diagonal matrices. In this case, we can redefine the problem as

$$A_\delta^{\mathcal{S}} \in A + \underset{\Delta \in \mathcal{S}}{\text{argmin}} \left\{ \|\Delta\|_F : \max_{D \in \Omega_m} \mu_2(D(A + \Delta)) = \delta \right\}. \quad (8)$$

The definitions (7) and (8) involve the solution of a matrix nearness problem that is the main effort of this paper. Notice that such matrix nearness problem is not convex, which means  $A_\delta$  and  $A_\delta^{\mathcal{S}}$  may not be unique since there could be multiple minimizers. However, in the numerical experiments in Section 5 we will consider the solution computed by the algorithm. Moreover, the choice of  $\delta$  as a positive constant of moderate size yields a computed matrix that is closer to the original weight matrix  $A$ .

We will address only the problem of computing  $A_\delta$ , but the proposed approach can be extended easily to compute  $A_\delta^{\mathcal{S}}$  by introducing the orthogonal projection onto  $\mathcal{S}$ .

## 2.1 A two-level method for the weight matrix stabilization

Our solution approach to compute  $A_\delta$  follows the methods presented in [25, 26] and their extensions [27, 28], and can be sketched as follows.

Given a target value  $\bar{\delta} \in \mathbb{R}$ , we aim to find a perturbation  $\Delta \in \mathbb{R}^{n,n}$  of minimal Frobenius norm such that

$$\max_{D \in \Omega_m} \mu_2(D(A + \Delta)) = \bar{\delta}.$$

If  $\max_{D \in \Omega_m} \mu_2(DA) \leq \bar{\delta}$ , then we simply set  $\Delta = 0$ , which implies  $A_\delta = A$ . Otherwise we proceed with the computation of  $\Delta$ , which we rewrite as  $\Delta = \varepsilon E$ , with

$$E \in \mathbb{S}_1 := \{E \in \mathbb{R}^{n,n} : \|E\|_F = 1\}$$

and where  $\varepsilon > 0$  denotes the perturbation size. We consider a two-level approach consisting of an *inner* and an *outer iteration*.

- **Inner iteration.** For a fixed  $\varepsilon$ , we solve the optimization problem

$$\min_{E \in \mathbb{S}_1} \nu_\varepsilon(E) =: f(\varepsilon), \quad (9)$$

where

$$\nu_\varepsilon(E) := \max_{D \in \Omega_m} \mu_2(D(A + \varepsilon E)). \quad (10)$$

We denote the minimizer of (9) as  $E_\star(\varepsilon)$ .

- **Outer iteration.** We solve the scalar equation with respect to  $\varepsilon$

$$f(\varepsilon) = \bar{\delta}, \quad (11)$$

and we tune the parameter  $\varepsilon$  by means of a Newton-like technique to solve the problem

$$\min\{\varepsilon > 0 : f(\varepsilon) = \bar{\delta}\}, \quad (12)$$

whose solution is denoted as  $\varepsilon_\star$ .

This yields a matrix  $A + \Delta_\star$ , with  $\Delta_\star = \varepsilon_\star E_\star(\varepsilon_\star)$ , such that

$$\nu_{\varepsilon_\star}(E_\star(\varepsilon_\star)) = \max_{D \in \Omega_m} \mu_2(D(A + \varepsilon_\star E_\star(\varepsilon_\star))) = \bar{\delta}.$$

This means that for the slightly modified matrix  $A + \Delta_\star$ , the logarithmic norm of  $D(A + \Delta_\star)$  is uniformly bounded from above by  $\bar{\delta}$ , independently of  $D \in \Omega_m$ .

Numerical experiments on the MNIST [29] and FashionMNIST [30] datasets show that neural networks with a one layer weight-tied neural ODE, trained using the proposed stabilization, are more robust against adversarial attacks than those trained using a classical approach, without sacrificing too much accuracy.

## 3 Inner iteration: minimizing the objective function

In this section, for a fixed  $\varepsilon > 0$ , we focus on the solution of the inner iteration optimization problem (9). In order to minimize  $\nu_\varepsilon(E)$  over all matrices  $E \in \mathbb{S}_1$ , by definition of logarithmic 2-norm (5), we aim to minimize the functional

$$F_\varepsilon(E) = \frac{1}{2} \sum_{i=1}^n (\lambda_i(\text{Sym}(D_\star(A + \varepsilon E))) - \bar{\delta})_+^2, \quad (13)$$

over all matrices  $E \in \mathbb{S}_1$ , with

$$D_\star = D_\star(\varepsilon, E) := \operatorname{argmax}_{D \in \Omega_m} \mu_2(D(A + \varepsilon E)). \quad (14)$$

Therefore the inner iteration consists in solving the following minimization problem

$$\min_{E \in \mathbb{S}_1} \frac{1}{2} \sum_{i=1}^n (\lambda_i(\operatorname{Sym}(D_\star(A + \varepsilon E))) - \bar{\delta})_+^2, \quad (15)$$

where the computation of  $D_\star$  has already been discussed in [27].

**Remark 3.1.** *The matrix  $D_\star$  is piecewise constant in  $\varepsilon$  and  $E$ , that is  $D_\star$  does not change for small variations of  $\varepsilon$  or  $E$ . Thus, from now on, we consider  $D_\star$  as a locally constant matrix with vanishing derivatives.*

We will derive a matrix differential equation whose stationary points are the local minima of the minimization problem (15). We then illustrate how to integrate the differential equation and we discuss the properties of its stationary points.

We will often use the following standard perturbation result for eigenvalues.

**Lemma 3.1.** [31, Section II.1.1] *Consider a continuously differentiable symmetric matrix valued function  $C : \mathbb{R} \rightarrow \mathbb{R}^{n,n}$ . Let  $\lambda(t)$  be a simple eigenvalue of  $C(t)$  for all  $t \in \mathbb{R}$  and let  $x(t)$  with  $\|x(t)\|_2 = 1$  be the associated (right and left) eigenvector. Then  $\lambda(t)$  is differentiable with*

$$\dot{\lambda}(t) = x(t)^\top \dot{C}(t)x(t) = \langle x(t)x(t)^\top, \dot{C}(t) \rangle_F.$$

Suppose that  $E$  is a smooth matrix valued function  $E(t)$  of the independent real variable  $t$  such that the eigenvalues  $\lambda_i(t)$  of  $\operatorname{Sym}(D_\star(A + \varepsilon E(t)))$  are simple, for all  $t$ , with corresponding unit eigenvectors  $x_i(t)$  and  $D_\star$  is defined in (14). Then, applying Lemma 3.1, yields

$$\dot{\lambda}_i(t) = \varepsilon x_i(t)^\top \left( \frac{D_\star \dot{E}(t) + \dot{E}(t)^\top D_\star}{2} \right) x_i(t) = \varepsilon \frac{x_i(t)^\top D_\star \dot{E}(t)x_i(t) + x_i(t)^\top \dot{E}(t)^\top D_\star x_i(t)}{2}.$$

Consequently, by omitting the dependence on  $t$  for conciseness, we have that

$$\frac{1}{\varepsilon} \frac{d}{dt} F_\varepsilon(E) = \sum_{i=1}^n \gamma_i \left( \frac{x_i^\top D_\star \dot{E} x_i + x_i^\top \dot{E}^\top D_\star x_i}{2} \right) = \sum_{i=1}^n \gamma_i z_i^\top \dot{E} x_i = \left\langle \sum_{i=1}^n \gamma_i z_i x_i^\top, \dot{E} \right\rangle_F,$$

with  $z_i(t) = D_\star x_i(t)$  and  $\gamma_i(t) = (\lambda_i(\operatorname{Sym}(D_\star(A + \varepsilon E(t)))) - \bar{\delta})_+$ . Dropping the irrelevant factor  $\varepsilon$ , which amounts to a rescaling of time, yields that the free gradient of  $F_\varepsilon(E)$  is

$$G_\varepsilon(E) = \sum_{i=1}^n \gamma_i z_i x_i^\top. \quad (16)$$

The admissible steepest descent direction  $\dot{E}$  of  $F_\varepsilon(E)$  must fulfill the constraint  $\|E(t)\|_F = 1$  and hence, as shown in [26, Lemma 2.6] and [32, Lemma 3.2], it has to be

$$\dot{E} = -G_\varepsilon(E) + \mu E, \quad \mu = \langle G_\varepsilon(E), E \rangle_F. \quad (17)$$

This yields a differential equation for  $E$  which, by construction, preserves the unit Frobenius norm of  $E(t)$ :

$$\frac{1}{2} \frac{d}{dt} \|E(t)\|_F^2 = \langle E, \dot{E} \rangle_F = \langle E, -G_\varepsilon(E) + \mu E \rangle_F = -\langle E, G_\varepsilon(E) \rangle_F + \mu \langle E, E \rangle_F = 0.$$

Moreover, equation (17) is a gradient system, i.e. along its solutions the functional  $F_\varepsilon(E(t))$  decays monotonically, since the constraint  $\|E\|_F = 1$  and the Cauchy-Schwarz inequality implies

$$\frac{1}{\varepsilon} \frac{d}{dt} F_\varepsilon(E(t)) = \langle G_\varepsilon(E), \dot{E} \rangle_F = \langle G_\varepsilon(E), -G_\varepsilon(E) + \mu E \rangle_F = -\|G_\varepsilon(E)\|_F^2 + \langle G_\varepsilon(E), E \rangle_F^2 \leq 0. \quad (18)$$

**Remark 3.2.** *Our approach is based on the eigenvalue perturbation formula of Lemma 3.1, which assumes that the eigenvalues are simple. However, this supposition is not restrictive since the subset of  $\mathbb{R}^{n,n}$  of matrices with multiple eigenvalues has zero measure [33] and, even if a continuous trajectory runs into a point with multiple eigenvalues, it is highly unlikely that the discretization of the differential equation captures it. Also, from the practical point of view, we experienced that the numerical integration is not affected by the coalescence of two or more eigenvalues. Thus, from here on, we assume that the eigenvalues of  $\text{Sym}(D_\star(A + \varepsilon E))$  are simple.*

The stationary points of (17) are characterized as follows.

**Theorem 3.1.** *Provided that there is at least an eigenvalue of  $\text{Sym}(D_\star(A + \varepsilon E))$  larger than  $\bar{\delta}$ , the following statements are equivalent along solutions of (17):*

1.  $\frac{d}{dt} F_\varepsilon(E(t)) = 0$ ;
2.  $\dot{E} = 0$ ;
3.  $E$  is a multiple of  $G_\varepsilon(E) = \sum_{i=1}^n \gamma_i z_i x_i^\top$ .

*Proof.* Let  $G = G_\varepsilon(E)$ , and recall that

$$\dot{E} = -G + \langle G, E \rangle_F E, \quad (19)$$

$$\frac{1}{\varepsilon} \frac{d}{dt} F_\varepsilon(E) = \langle G, \dot{E} \rangle_F. \quad (20)$$

Equation (19) and  $\|E\|_F = 1$  yields that statement 3 implies statement 2, while equation (20) yields that statement 2 implies statement 1. So it remains to show that statement 1 implies statement 3. Since  $G$  is non zero because we have assumed that at least an eigenvalue is larger than  $\bar{\delta}$ , inequality (18) is strict unless  $G$  is a real multiple of  $E$ . Hence, statement 3 implies statement 1.  $\square$

In Algorithm 1 we provide a schematic description of a single step of the numerical integration of equation (17). We make use of the Euler method, but considering other explicit methods could also be possible.

### 3.1 Simplification of the inner iteration

We use the notation that for a vector  $d \in \mathbb{R}^n$ ,  $D = \text{diag}(d) \in \mathbb{R}^{n,n}$  indicates the diagonal matrix with  $d$  in the diagonal and viceversa for a matrix  $D \in \mathbb{R}^{n,n}$ ,  $\text{diagvec}(D) \in \mathbb{R}^n$  denotes the vector formed by its diagonal. We notice that after the  $k$ -th step of the Euler method, with  $k > 0$ , for equation (17), namely lines 2 and 9 in Algorithm 1, the matrix

$$D_\star^{(k)} = \underset{D \in \Omega_m}{\text{argmax}} \mu_2(D(A + \varepsilon E_k))$$

has to be updated.



---

**Algorithm 1:** Integration step from  $t_k$  to  $t_{k+1}$  for the constrained gradient system (with  $\varepsilon$  fixed)

---

**Data:**  $A, E_k \approx E(t_k), f_k = F_\varepsilon(E_k), h_k$  (proposed step size),  $\varepsilon, \theta > 1$

**Result:**  $E_{k+1} \approx E(t_{k+1}), h_{k+1}$

**begin**

```

1   Initialize the step size by the proposed one,  $h = h_k$ 
2   Compute  $D_\star^{(k)} = \operatorname{argmax}_{D \in \Omega_m} \mu_2(D(A + \varepsilon E_k))$ 
3   Compute the eigenpairs  $(\lambda_i, x_i), \lambda_i > \bar{\delta}$  and  $\|x_i\|_2 = 1$ , of  $\operatorname{Sym}(D_\star^{(k)}(A + \varepsilon E_k))$ 
4   Compute  $z_i = D_\star^{(k)} x_i$ 
5   Compute the gradient  $G_k \approx G_\varepsilon(E(t_k))$  according to (16)
6   Compute  $\dot{E}_k \approx \dot{E}(t_k)$  according to (17)
7   Initialize  $f(h) = f_k$  and  $\text{reject} = 0$ 
8   Set  $E(h) = E_k + h\dot{E}_k$ , and  $E(h) = \frac{E(h)}{\|E(h)\|_F}$ 
   while  $f(h) \geq f_k$  do
9     Compute  $D_\star(h) = \operatorname{argmax}_{D \in \Omega_m} \mu_2(D(A + \varepsilon E(h)))$ 
10    Compute the eigenpairs  $(\lambda_i, x_i), \lambda_i > \bar{\delta}$  and  $\|x_i\|_2 = 1$ , of
         $\operatorname{Sym}(D_\star(h)(A + \varepsilon E(h)))$ , and set  $f(h) = F_\varepsilon(E(h))$ 
   if  $f(h) \geq f_k$  then
11     Reduce the step size,  $h := h/\theta$ 
12     Set  $E(h) = E_k + h\dot{E}_k$ , and  $E(h) = \frac{E(h)}{\|E(h)\|_F}$ 
        Set  $\text{reject} = 1$ 
   if  $\text{reject} = 0$  then
     Set  $h_{\text{next}} := \theta h$ 
   else
     Set  $h_{\text{next}} := h$ 
13  Set the starting values for the next step:  $E_{k+1} = E(h)$ , and  $h_{k+1} = h_{\text{next}}$ 
   return

```

---

We let  $d_\star^{(k)} = \operatorname{diag}(D_\star^{(k)})$ . Computing  $d_\star^{(k+1)}$  (equivalently the matrix  $D_\star^{(k+1)}$ ) requires the integration of a constrained gradient system, see [27], and thus, the overall exact integration of equation (17) would be expensive. In order to avoid this, we try to approximate  $d_\star^{(k+1)}$  by exploiting the property, which we expect, that its entries are either  $m$  or 1 (see [27, Theorem 3.1]).

We now formalize how this approximation is carried out. Given  $E_k \approx E(t_k)$  and  $D_\star^{(k)}$ , we need to approximate

$$D_\star^{(k+1)} = \operatorname{argmax}_{D \in \Omega_m} \mu_2(D(A + \varepsilon E_{k+1})), \quad (21)$$

where  $E_{k+1} \approx E(t_{k+1})$ . Instead of integrating the constrained gradient system in [27, Section 3] for  $d = \operatorname{diagvec}(D)$ , that is

$$\dot{d} = g := \operatorname{diagvec}(\operatorname{Sym}(zx^\top)), \quad (22)$$

where  $x$  is the eigenvector associated with the largest eigenvalue of  $\operatorname{Sym}(D(A + \varepsilon E_{k+1}))$  and  $z = (A + \varepsilon E_{k+1})x$ , we use a semi-combinatorial approach.

We aim to compute a solution  $D_\star = \operatorname{diag}(d_\star)$  of (21) as follows. We start setting  $d^{[0]} = d_\star^{(k)}$

and then we update it according to the following iterative process starting from  $\ell = 0$ :

$$\left(d^{[\ell+1]}\right)_i = \begin{cases} 1 & \text{if } (g^{[\ell]})_i > 0 \\ m & \text{if } (g^{[\ell]})_i < 0 \end{cases}, \quad (23)$$

where  $g^{[\ell]}$  is the gradient defined in (22) for  $D = \text{diag}(d^{[\ell]})$ . If, for some  $\ell$ , it occurs that  $d^{[\ell+1]} = d^{[\ell]}$ , the iteration stops,  $d^{[\ell]}$  is the sought solution and  $D_\star^{(k+1)} = \text{diag}(d^{[\ell]})$ .

The idea behind (23) is that, given the constraint that the entries of  $d$  are bounded from below by  $m$  and from above by 1,  $d^{[\ell]}$  is optimal if in correspondence of its maximal entries (equal to 1), the gradient is positive, and in correspondence with its minimal entries (equal to  $m$ ), the gradient is negative. The number of iterations *maxit* we perform is typically small (20 at most in our experiments).

The iterative method is outlined in Algorithm 2.

---

**Algorithm 2:** Iteration to update  $D_\star^{(k+1)} = \text{diag}(d_\star^{(k+1)})$

---

**Data:**  $A, d_\star^{(k)}, E_{k+1} \approx E(t_{k+1}), \varepsilon, \text{maxit}$  (default 20)

**Result:**  $d_\star^{(k+1)}$

**begin**

```

1   Set  $\ell = 0, d^{[\ell]} = d_\star^{(k)}$  and  $Stop = False$ 
   while  $\ell < \text{maxit}$  and  $Stop = False$  do
2     Define  $d^{[\ell+1]}$  as the update of  $d^{[\ell]}$  according to (23)
3     Compute the eigenvector  $x^{[\ell+1]}$  associated with the largest eigenvalue of
        $\text{Sym}(D^{[\ell+1]}(A + \varepsilon E_{k+1}))$ 
4     Compute  $z^{[\ell+1]} = (A + \varepsilon E_{k+1})x^{[\ell+1]}$ 
5     Compute the approximate gradient  $g^{[\ell+1]} = \text{diagvec}(\text{Sym}(z^{[\ell+1]}(x^{[\ell+1]})^\top))$ 
6     Check the sign of the approximate gradient  $g^{[\ell+1]}$  according to (23) and set
        $Stop = True$  if  $d^{[\ell+1]} = d^{[\ell]}$ 
7     Set  $\ell = \ell + 1$ 
   if  $\ell < \text{maxit}$  then
8     Set  $d_\star^{(k+1)} = d^{[\ell]}$ 
   else
9     Compute  $D_\star^{(k+1)}$  by integrating the constrained gradient system in (22)
   return

```

---

### 3.1.1 Illustrative example

Consider the matrix

$$A = \begin{pmatrix} -0.39 & -1.16 & 0.74 \\ 1.14 & 0.96 & 0.15 \\ 0.42 & -0.14 & -2.32 \end{pmatrix}$$

and the perturbation  $\varepsilon E(t)$  with  $\varepsilon = 0.3$  and

$$E(t) = \nu(t) \begin{pmatrix} -\sin(2t)/2 & \sin(t^2) & t \\ -t/4 & -t & \sin(t/2) \\ -\sin(t)^2 & \cos(t) & t \end{pmatrix},$$

being  $\nu(t) = \|E(t)\|_F^{-1}$ .

We fix  $m = 0.5$  and compute  $\mu(t) = \mu(D(t)(A + \varepsilon E(t)))$  in the time interval  $[0, 1]$  where  $D(t)$  is the local extremizer computed by our algorithm. Figure 1 illustrates the descendent behaviour of  $\mu(t)$ . We use a discretization stepsize  $h = 0.05$  and solve the optimization problem by the simplified inner iteration.

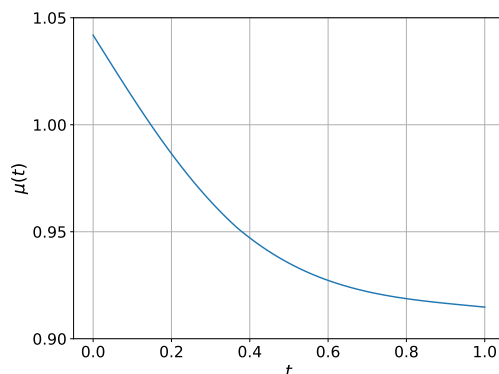


Figure 1: Behaviour of  $\mu(t) = \mu(D(t)(A + \varepsilon E(t)))$  as  $t \in [0, 1]$ .

For  $t \leq 0.3$  the extremizer is  $D_1 = \text{diag}(m \ 1 \ 1)$ . At  $t = 0.45$ , the extremizer ceases to exist since the gradient is

$$G = (-0.2865 \quad 1.0832 \quad -0.0002)^\top,$$

due to the negativity of last entry. At this point, shifting the last entry of  $D$  from  $m$  to 1 gives the candidate extremizer  $D_2 = \text{diag}(m \ 1 \ m)$ . The corresponding gradient is

$$G = (-0.2804 \quad 1.0830 \quad -0.0043)^\top,$$

which satisfies the necessary condition for extremality so that  $D_2$  is indeed an extremizer. From now on, that is for all  $t \geq 0.45$ ,  $D_2$  remains an extremizer. However, we note that for  $t \in [0.35, 0.45]$  both  $D_1$  and  $D_2$  are extremizers although our algorithm detects only the transition at  $t = 0.45$  when  $D_2$  becomes the unique extremizer.

### 3.2 Two layer vector field

In this case, the vector field is a two-layer neural network

$$f(x) = \sigma(A_2 \sigma(A_1 x + b_1) + b_2), \quad x \in \mathbb{R}^n,$$

using the Lagrange theorem, for any two vectors  $x$  and  $y$ , we get

$$f(x) - f(y) = \text{diag}(\sigma'(u_2)) A_2 \text{diag}(\sigma'(u_1)) A_1 (x - y) = D_2 A_2 D_1 A_1 (x - y),$$

with  $D_i = \text{diag}(\sigma'(u_i))$ , for suitable vectors  $u_1, u_2$ . Therefore, with computations analogous to the one layer case, we obtain that the neural ODE (1) satisfies the one-sided Lipschitz condition

$$\langle f(x) - f(y), x - y \rangle_2 \leq \delta \|x - y\|_2^2, \quad x, y \in \mathbb{R}^n,$$

with

$$\delta := \max_{D_1, D_2 \in \Omega_m} \mu_2(D_2 A_2 D_1 A_1).$$

Given  $\bar{\delta} \in \mathbb{R}$ ,  $\bar{\delta} < \delta$ , the goal is now the computation of the smallest matrices  $\Delta_1, \Delta_2$  in Frobenius norm such that

$$\max_{D_1, D_2 \in \Omega_m} \mu_2(D_2(A_2 + \Delta_2)D_1(A_1 + \Delta_1)) = \bar{\delta}.$$

In the following, we will write  $\Delta_i = \varepsilon_i E_i$ , for  $i = 1, 2$ , with  $E_i$  a matrix of unit Frobenius norm and  $\varepsilon_i$  its amplitude. For simplicity of presentation, we are assuming  $\varepsilon_1 = \varepsilon_2 = \varepsilon$ .

Fixed  $\varepsilon > 0$ , the minimization problem (15) becomes

$$\min_{E_1, E_2 \in \mathbb{S}_1} F_\varepsilon(E_1, E_2), \quad \text{with } F_\varepsilon(E_1, E_2) = \frac{1}{2} \sum_{i=1}^n (\lambda_i(\text{Sym}(D_\star^1(A_1 + \varepsilon E_1)D_\star^2(A_2 + \varepsilon E_2)) - \bar{\delta}))_+^2,$$

where

$$(D_\star^1, D_\star^2) = \operatorname{argmax}_{D_1, D_2 \in \Omega_m} \mu_2(D_2(A_2 + \varepsilon E_2)D_1(A_1 + \varepsilon E_1)).$$

Applying Lemma 3.1 to  $F_\varepsilon(E_1, E_2)$ , with  $E_i = E_i(t)$  for  $i = 1, 2$ , yields

$$\frac{1}{\varepsilon} \frac{d}{dt} F_\varepsilon(E_1(t), E_2(t)) = \left\langle \dot{E}_1, \sum_{i=1}^n \gamma_i z_i^1 (w_i^1)^\top \right\rangle_F + \left\langle \dot{E}_2, \sum_{i=1}^n \gamma_i z_i^2 (w_i^2)^\top \right\rangle_F,$$

where  $\gamma_i = (\lambda_i(\text{Sym}(D_\star^1(A_1 + \varepsilon E_1)D_\star^2(A_2 + \varepsilon E_2)) - \bar{\delta}))_+$ ,  $x_i$  is the unit eigenvector corresponding to the eigenvalue  $\lambda_i(\text{Sym}(D_\star^1(A_1 + \varepsilon E_1)D_\star^2(A_2 + \varepsilon E_2)))$ , and

$$\begin{aligned} z_i^1 &= D_\star^1(A_2 + \varepsilon E_2(t))^\top D_\star^2 x_i, & w_i^1 &= x_i, \\ z_i^2 &= D_\star^2 x_i, & w_i^2 &= D_\star^1(A_1 + \varepsilon E_1(t)) x_i. \end{aligned}$$

Therefore, for  $k = 1, 2$ , the free gradients of  $F_\varepsilon$  with respect to  $E_k$  are

$$G_k = \sum_{i=1}^n \gamma_i z_i^k (w_i^k)^\top,$$

and the associated constrained gradient systems are

$$\dot{E}_k = -G_k + \langle G_k, E_k \rangle_F E_k. \quad (24)$$

## 4 Outer iteration: tuning the size of the perturbation

In this section, we focus on the solution of the outer iteration optimization problem (12). We let  $E_\star(\varepsilon)$  of unit Frobenius norm be a local minimizer of the inner iteration (9), and we denote by  $\lambda_i(\varepsilon)$  and  $x_i(\varepsilon)$ , for  $i = 1, \dots, n$ , the eigenvalues and unit eigenvectors of  $\text{Sym}(D_\star(A + \varepsilon E_\star(\varepsilon)))$ . We denote by  $\varepsilon_\star$  the smallest value of  $\varepsilon$  such that  $F_{\varepsilon_\star}(E_\star(\varepsilon_\star)) = 0$ . From the Schur normal form of  $\text{Sym}(DA)$ , it is trivial to construct a diagonal perturbation of the diagonal Schur factor that shifts the eigenvalues larger than  $\bar{\delta}$  to the value of  $\bar{\delta}$ . Hence, it follows that  $\varepsilon_\star$  exists, with

$$\varepsilon_\star \leq \left( \sum_{i=1}^n (\lambda_i(\text{Sym}(D_\star A)) - \bar{\delta})_+^2 \right)^{\frac{1}{2}}.$$

To determine  $\varepsilon_\star$ , we are thus left with a one-dimensional root-finding problem, for which a variety of standard methods, such as bisection and the like, could be employed. In the following we derive a Newton-like algorithm, for which we need to impose an extra assumption.

**Assumption 4.1.** For  $\varepsilon < \varepsilon_*$ , we assume that the eigenvalues  $\lambda_i(\varepsilon)$  of  $\text{Sym}(D_*(A + \varepsilon E_*(\varepsilon)))$  are simple. Moreover,  $E_*(\varepsilon)$ ,  $\lambda_i(\varepsilon)$  and  $x_i(\varepsilon)$  are assumed to be smooth functions of  $\varepsilon$ .

**Remark 4.1.** Assumption 4.1 is important because, if this is not satisfied, the standard derivative formula for simple eigenvalues 3.1, which we use, would not hold. In principle, this assumption limits the set of matrices that the algorithm is able to stabilize, since there will be cases where the closest stabilized matrix has multiple eigenvalues. But, such matrices form a subset of  $\mathbb{R}^{n,n}$  with zero measure [33], so this is a nongeneric situation.

For  $\varepsilon < \varepsilon_*$ , the following result provides a cheap formula for the computation of the derivative of  $f(\varepsilon) = F_\varepsilon(E_*(\varepsilon))$ , which is the basic tool in the construction of the outer iteration of the method. This is expressed in terms of the free gradient of  $F_\varepsilon$  at  $E_*(\varepsilon)$ :

$$G(\varepsilon) = \sum_{i=1}^n \gamma_i(\varepsilon) z_i(\varepsilon) x_i(\varepsilon)^\top,$$

with  $\gamma_i(\varepsilon) = (\lambda_i(\text{Sym}(D_*(A + \varepsilon E_*(\varepsilon)))) - \bar{\delta})_+$  and  $z_i(\varepsilon) = D_* x_i(\varepsilon)$ .

**Lemma 4.1.** For  $\varepsilon < \varepsilon_*$ , under Assumption 4.1, the function  $f(\varepsilon) = F_\varepsilon(E_*(\varepsilon))$  is differentiable, and its derivative equals

$$f'(\varepsilon) = -\|G(\varepsilon)\|_F. \quad (25)$$

*Proof.* See [25, Lemma 3.5]. □

## 4.1 An algorithm to approximate the size of the perturbation

Since the eigenvalues are assumed to be simple, the function  $f(\varepsilon)$  has a double zero at  $\varepsilon_*$  because it is a sum of squares, and hence it is convex for  $\varepsilon \leq \varepsilon_*$ . This means that we may approach  $\varepsilon_*$  from the left by the classical Newton iteration

$$\varepsilon_{k+1} = \varepsilon_k - \frac{f(\varepsilon_k)}{f'(\varepsilon_k)}, \quad k = 0, 1, \dots$$

which is such that  $|\varepsilon_{k+1} - \varepsilon_*| \approx \frac{1}{2} |\varepsilon_k - \varepsilon_*|$  and  $\varepsilon_{k+1} < \varepsilon_*$  if  $\varepsilon_k < \varepsilon_*$ .

The estimate  $|\varepsilon_{k+1} - \varepsilon_*| \approx \frac{1}{2} |\varepsilon_k - \varepsilon_*|$  is due to the fact that the Newton method is applied to a function with a double zero. The convexity of the function to the left of  $\varepsilon_*$  guarantees the monotonicity of the sequence and its boundedness.

In Algorithm 3 we illustrate how the inner level and the outer level of our optimization approach have to be combined in order to get the desired approximation of  $\varepsilon_*$ . It is important in lines 1 and 4 to choose properly the initial datum of the constrained gradient system (17) integration in order to get the best performance of the algorithm.

- At perturbation size  $\varepsilon_0$ , the initial datum is simply chosen to be the opposite of the normalized gradient  $-G_{\varepsilon_0}(E)/\|G_{\varepsilon_0}(E)\|_F$  of the functional (13) evaluated at  $E = 0$ , the zero matrix.
- At perturbation size  $\varepsilon_{k+1}$ , for  $k \geq 0$ , the initial datum is computed in the following way. Given a minimum  $E(\varepsilon_k)$  at perturbation size  $\varepsilon_k$ , the free gradient system

$$\dot{E}(t) = -G(E(t)), \quad t \geq 0, \quad (26)$$

with initial datum  $E(0) = \varepsilon_k E(\varepsilon_k)$ , is solved numerically until  $\|E(t)\|_F = \varepsilon_{k+1}$ . The result of the numerical integration is then normalized in Frobenius norm and set as the initial

---

**Algorithm 3:** Basic algorithm for approximating  $\varepsilon_*$ 

---

**Data:** A tolerance  $\text{tol} > 0$  and an initial  $\varepsilon_0 < \varepsilon_*$

**Result:**  $\varepsilon_*$  and  $E(\varepsilon_*)$

**begin**

- 1    Integrate the constrained gradient system (17) with fixed perturbation size  $\varepsilon_0$
  - 2    Compute  $f_0 = f(\varepsilon_0)$  and  $f'_0 = f'(\varepsilon_0)$  as in (11) and (25), and set  $k = 0$
  - while**  $f_k \geq \text{tol}$  **do**
  - 3     Set  $\varepsilon_{k+1} = \varepsilon_k - \frac{f_k}{f'_k}$
  - 4     Integrate the constrained gradient system (17) with fixed perturbation size  $\varepsilon_{k+1}$
  - 5     Compute  $f_{k+1} = f(\varepsilon_{k+1})$  and  $f'_{k+1} = f'(\varepsilon_{k+1})$  as in (11) and (25), and set  
       $k = k + 1$
  - 6    Set  $\varepsilon_* = \varepsilon_k$  and  $E(\varepsilon_*) = E(\varepsilon_k)$
  - return**
- 

datum of the constrained gradient system (17) integration at perturbation size  $\varepsilon_{k+1}$ . This choice guarantees the overall continuity of the functional (13) throughout its minimization at different perturbation sizes  $\varepsilon$ , which is essential to get the best performance of the overall procedure.

The gradient system (26) is integrated with the Euler method – other explicit methods could also be used – with constant step size  $h$ :

$$E_{\ell+1} = E_\ell - hG(E_\ell), \quad \ell = 0, 1, \dots$$

At each integration step, the norm of the matrix  $E(t)$  increases in order to move the eigenvalues below  $\bar{\delta}$ , that is  $\|E_\ell\|_F < \|E_{\ell+1}\|_F$ , for  $\ell \geq 0$ . Therefore the numerical integration is stopped when  $\|E_{\ell^*+1}\|_F \geq \varepsilon_{k+1}$  for some  $\ell^*$ , and the last integration step size is tuned using the Newton method to get the equality. This is achieved as follows.

We define the function

$$g(h) = \|E_{\ell^*+1}\|_F^2 - \varepsilon_{k+1}^2 = \|E_{\ell^*} - hG(E_{\ell^*})\|_F^2 - \varepsilon_{k+1}^2,$$

and we aim to find its root  $h^*$  such that  $g(h^*) = 0$ . Its derivative is simply

$$g'(h) = -2 \sum_{i,j=1}^n (E_{\ell^*} - hG(E_{\ell^*}))_{ij} G(E_{\ell^*})_{ij}.$$

Then, starting from  $h_0 = h/2$ , we perform the Newton method

$$h_{i+1} = h_i - \frac{g(h_i)}{g'(h_i)}, \quad i = 0, 1, \dots$$

until we get the sought  $h^*$  and, consequently,  $E_{\ell^*+1} = E_{\ell^*} - h^*G(E_{\ell^*})$ . Eventually,  $E_{\ell^*+1}$  is normalized in Frobenius norm and set as the initial datum of the constrained gradient system (17) integration at perturbation size  $\varepsilon_{k+1}$ .

## 4.2 Extension to the two layer vector field

We denote by  $E_*^1(\varepsilon), E_*^2(\varepsilon)$  the stationary points of the gradient systems (24) and we look for the smallest zero  $\varepsilon_*$  of

$$f(\varepsilon) = F_\varepsilon(E_*^1(\varepsilon), E_*^2(\varepsilon)).$$

As in the one layer case, to determine  $\varepsilon_*$ , we are left with a one-dimensional root-finding problem, for which we derive a Newton-like algorithm. We suppose that the following assumption, analogous to Assumption 4.1, holds.

**Assumption 4.2.** *For  $\varepsilon < \varepsilon_*$ , we assume that the eigenvalues  $\lambda_i(\varepsilon)$  of  $D_*^2(A_2 + \varepsilon E_*^2(\varepsilon))D_*^1(A_1 + \varepsilon E_*^1(\varepsilon))$  are simple. Moreover,  $E_*^k(\varepsilon)$ ,  $\lambda_i(\varepsilon)$  and the associated unit eigenvectors  $x_i(\varepsilon)$  are assumed to be smooth functions of  $\varepsilon$ .*

If  $G_1(\varepsilon), G_2(\varepsilon)$  are the gradients of  $F_\varepsilon$  with respect to  $E_*^1(\varepsilon), E_*^2(\varepsilon)$ , then we have a result analogous to Lemma 4.1.

**Lemma 4.2.** *For  $\varepsilon < \varepsilon_*$ , under Assumption 4.2, the function  $f(\varepsilon) = F_\varepsilon(E_*^1(\varepsilon), E_*^2(\varepsilon))$  is differentiable, and its derivative equals*

$$f'(\varepsilon) = -(\|G_1(\varepsilon)\|_F + \|G_2(\varepsilon)\|_F).$$

## 5 Numerical experiments

To conclude, we apply the theory developed in the previous sections to increase the robustness of a neural network image classifier that includes a neural ODE in its architecture. To this end, we consider MNIST dataset [29] and FashionMNIST dataset [30] perturbed via the Fast Gradient Sign Method (FGSM) adversarial attack [6].

Recall that MNIST and FashionMNIST consist of 70000  $28 \times 28$  grayscale images (60000 training images and 10000 testing images), that is vectors of length 784 after vectorization. We consider a neural network made up of the following blocks:

- (a) a downsampling affine layer that reduces the dimension of the input from 784 to 64, i.e. a simple transformation of the kind  $y = A_1x + b_1$ , where  $x \in \mathbb{R}^{784}$  is the input,  $y \in \mathbb{R}^{64}$  is the output, and  $A_1 \in \mathbb{R}^{64,784}$  and  $b_1 \in \mathbb{R}^{64}$  are the parameters;
- (b) a neural ODE block that models the feature propagation,

$$\begin{cases} \dot{x}(t) = \sigma(Ax(t) + b), & t \in [0, 1], \\ x(0) = y, \end{cases}$$

whose initial value is the output of the previous layer, where  $x(t) : [0, 1] \rightarrow \mathbb{R}^{64}$  is the feature vector evolution function,  $A \in \mathbb{R}^{64,64}$  and  $b \in \mathbb{R}^{64}$  are the parameters, and  $\sigma$  is a custom activation function, defined as

$$\sigma(x) = \begin{cases} x, & \text{if } x \geq 0, \\ \tanh x, & \text{if } -\bar{x} \leq x < 0, \\ \alpha x + \beta, & \text{otherwise,} \end{cases}$$

where  $\bar{x} > 0$  is such that  $\tanh'(\pm\bar{x}) = \alpha = 0.1$  and  $\beta \in \mathbb{R}$  such that  $\alpha(-\bar{x}) + \beta = \tanh(-\bar{x})$  (see Figure 2);

- (c) a final classification layer that reduces the dimension of the input from 64 to 10, followed by the softmax activation function

$$x_{\text{out}} = \text{softmax}(A_2x(1) + b_2),$$

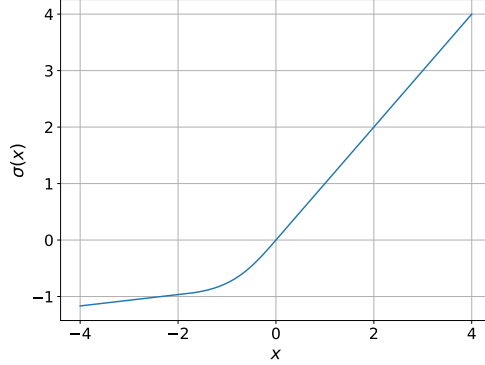


Figure 2: Custom activation function: a smoothed Leaky Rectified Linear Unit (LeakyReLU) with minimal slope  $\alpha = 0.1$ .

where  $x(1) \in \mathbb{R}^{64}$  is the output of the neural ODE block,  $A_2 \in \mathbb{R}^{10,64}$  and  $b_2 \in \mathbb{R}^{10}$  are the parameters, and  $x_{\text{out}}$  is the output vector whose component  $i$  is the probability that the input  $x$  belongs to the class  $i$ . Recall that softmax is a vector-valued function that maps the vector  $x$  into the vector  $\text{softmax}(x) = e^x / \|e^x\|_1$ , where exponentiation is done entrywise.

If we call  $\ell_1$  the transformation at point (a),  $\phi_1$  the flow of the differential equation at point (b) at time 1, and  $\ell_2$  the transformation at point (c), then the neural network model  $\phi$  can be written as

$$\phi = \ell_2 \circ \phi_1 \circ \ell_1 = \text{softmax}(A_2 \phi_1(A_1 \bullet + b_1) + b_2),$$

and it is easy to show that for any vectors  $x, y$

$$\|\phi(x) - \phi(y)\|_2 \leq L_{\text{softmax}} \|A_2\|_2 L_{\phi_1} \|A_1\|_2 \|x - y\|_2,$$

where  $L_{\text{softmax}}$  and  $L_{\phi_1}$  are the Lipschitz constants of softmax and  $\phi_1$  respectively. It is easy to show that  $L_{\text{softmax}} = 1$ , and that

$$L_{\phi_1} \leq \exp\left(\max_{D \in \Omega_m} \mu_2(DA)\right).$$

If we set  $\|A_1\|_2 = \|A_2\|_2 = 1$ , then

$$\|\phi(x) - \phi(y)\|_2 \leq L_{\phi_1} \|x - y\|_2 \leq \exp\left(\max_{D \in \Omega_m} \mu_2(DA)\right) \|x - y\|_2,$$

i.e. the Lipschitz constant of our model  $\phi$  is bounded by  $\exp(\max_{D \in \Omega_m} \mu_2(DA))$ , that we are able to tune as we like thanks to our two-level method. In particular, setting it equal to a constant of moderate size larger than 1, we make sure that small perturbations in input yield only small changes in output. This increases the robustness of the model  $\phi$  without sacrificing too much accuracy.

We now build two alternative versions of the above-mentioned model on MNIST and on FashionMNIST datasets.



- We train the first one by using the classical stochastic gradient descent for 70 epochs leading to the classical model, and we call it **ODEnet** from here on.
- Then, we build the second version of the model as follows.
  1. We retain the parameters of the classical one and we apply the two-level method to the weight matrix  $A$  in (b) to realize the condition  $\exp(\max_{D \in \Omega_m} \mu_2(DA)) > 1$  of moderate size. Specifically, given our target  $\bar{\delta} = \max_{D \in \Omega_m} \mu_2(DA) \geq 0$ , we compute  $\varepsilon_\star > 0$  and  $E_\star(\varepsilon_\star) \in \mathbb{S}_1$  such that

$$\hat{A} = A + \varepsilon_\star E_\star(\varepsilon_\star) \quad (27)$$

realizes the condition  $\mu_2(D_\star \hat{A}) = \bar{\delta}$ .

2. Once fixed the parameter  $\hat{A}$  in place of  $A$  in (b), we train the second version of the model by computing all other parameters by means of the classical stochastic gradient descent for 70 epochs.

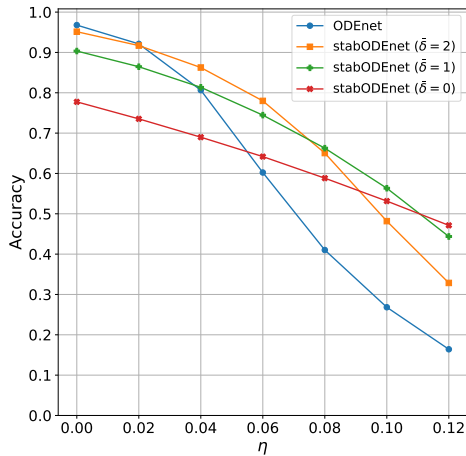
This is the stabilized model, and we call it **stabODEnet** from here on, where the prefix **stab** stands for stabilized.

We notice that the training time of the stabilized model is approximately twice as much the training time of the classical model. Indeed, the stabilized model is built on the classical model, so first we need to train the classical model using the stochastic gradient descent for 70 epochs. Then we perform the operation in (27) and eventually we train the stabilized model using the stochastic gradient descent for 70 epochs. So the only additional cost is given by the computation of  $E_\star(\varepsilon_\star)$  in (27). The cost of such operation depends on the size of the matrix  $A$ : the larger the size, the higher the cost of the operation. In our setting, where  $A \in \mathbb{R}^{64,64}$ , the computation of  $E_\star(\varepsilon_\star)$  in (27) takes few seconds, so its time is negligible compared to the training time, and we can say that the training time of the stabilized model is twice as much the training time of the classical model. Instead, for a very large matrix, for instance  $A \in \mathbb{R}^{1000,1000}$ , the computation of  $E_\star(\varepsilon_\star)$  in (27) takes about a few minutes, so we can say that the training time of the stabilized model is approximately twice as much the training time of the classical model.

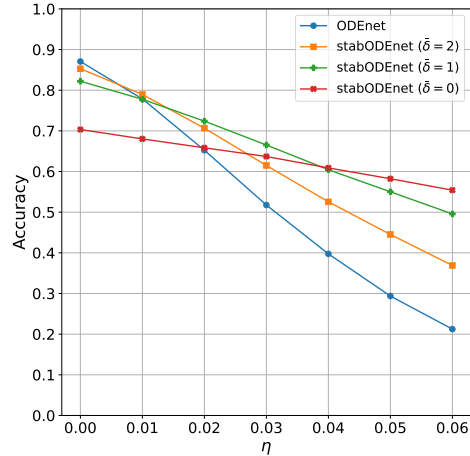
In our experiments, we compare the test accuracy of the models, i.e. the percentage of correctly classified testing images as a function of a perturbation  $0 < \eta \ll 1$ . Here, we define the parameter  $\eta$  as the size in the  $L^\infty$ -norm of the FGSM perturbation to each testing image, i.e. if the vector  $x$  is a testing image and  $\delta x$  is the unit infinity norm FGSM attack to  $x$ , then  $x + \eta \delta x$  is the resulting perturbed testing image.

## 5.1 Trade-off between accuracy and robustness

In this paragraph, we observe the behaviour of our model **stabODEnet** for different values of the parameter  $\bar{\delta}$  in relation to the unconstrained model **ODEnet**. In Figure 3, we plot the accuracy of **ODEnet** and **stabODEnet** for  $\bar{\delta} \in \{0, 1, 2\}$  as a function of the magnitude  $\eta$  of the FGSM adversarial attack. As  $\bar{\delta}$  increases, the model **stabODEnet** gains in accuracy, but it loses in robustness and stability. Figure 3 shows how the accuracy curves of **stabODEnet** approach the accuracy curve of **ODEnet** as  $\bar{\delta}$  increases. In contrast, as  $\bar{\delta}$  decreases, the model's robustness and stability improve, but its accuracy deteriorates. Hence, despite a reasonable drop in accuracy, the model **stabODEnet** is more reliable.



(a) MNIST dataset.



(b) FashionMNIST dataset.

Figure 3: Comparison of test accuracy across different models as a function of the magnitude  $\eta$  of the FGSM adversarial attack.

## 5.2 Comparison with other state-of-the-art models

Now we compare our approach with other state-of-the-art models in the literature. In particular, we consider the following approaches:

- the model proposed in Kang et al. [18], where the authors design a neural ODE whose equilibrium points correspond to the classes of the considered classification problem. By ensuring that the equilibrium points are Lyapunov-stable, the solution for a small perturbed input converges to the same solution for the unperturbed one. Furthermore, the authors choose the matrix  $A_2$  in (c) in such a way that it minimizes the maximum cosine similarity between the representations from two different classes. These choices of neural ODE in (b) and matrix  $A_2$  in (c) make the model robust to adversarial attacks. Since we cannot choose the neural ODE in (b) as in [18] – it is a different neural ODE than the one we consider, so the comparison with our model would not be fair – we choose only  $A_2$  in (c) as in [18], and we call this model from here on **KangODEnet**;
- the structured neural ODE proposed in Haber et al. [9], Ruthotto et al. [11], Celledoni et al. [23] and Ferdia et al. [24]

$$\dot{x}(t) = -A^\top \sigma(Ax(t) + b), \quad t \in [0, 1],$$

that is nonexpansive by construction and therefore robust to adversarial attacks. We call from here on **nsdODEnet** the model with such neural ODE in (b), where the prefix **nsd** stands for the fact that its Jacobian matrix is negative semi-definite;

- the neural ODE in (b) whose weight matrix  $A$  is stabilized by adding a perturbation  $\Delta$  that is chosen to be a suitable multiple of the identity matrix as in [27]. We call from here on **shiftODEnet** the model stabilized with such approach, i.e. with a shifting of a multiple of the identity matrix. It is worth noticing that the purpose of the paper [27] is not the

optimal stabilization of the weight matrix  $A$  in (b), so this approach is only illustrative and reported for a further comparison.

In Table 1 we report the results for the MNIST dataset and in Table 2 those for the FashionMNIST dataset. For `stabODEnet_d`, the perturbation  $E_*(\varepsilon_*) \in \mathbb{S}_1 \cap \mathbb{D}^{64,64}$  is set to be a diagonal matrix. We notice that `nsdODEnet` and `shiftODEnet` behave approximately as `stabODEnet` with  $\bar{\delta} = 0$ , as expected since they both are nonexpansive models.

$\eta$	0	0.02	0.04	0.06	0.08	0.10	0.12
ODEnet	0.9678	0.9212	0.8065	0.6023	0.4102	0.2683	0.1641
KangODEnet	<b>0.9794</b>	<b>0.9465</b>	<b>0.8802</b>	0.7478	0.5679	0.4062	0.2792
nsdODEnet	0.7941	0.7551	0.7091	0.6607	0.6084	0.5483	<b>0.4865</b>
stabODEnet ( $\bar{\delta} = 2$ )	0.9514	0.9170	0.8626	<b>0.7799</b>	0.6505	0.4818	0.3286
stabODEnet_d ( $\bar{\delta} = 2$ )	0.9448	0.9097	0.8545	0.7682	0.6473	0.4848	0.3412
stabODEnet ( $\bar{\delta} = 1$ )	0.9035	0.8646	0.8135	0.7446	<b>0.6627</b>	<b>0.5634</b>	0.4437
stabODEnet_d ( $\bar{\delta} = 1$ )	0.8823	0.8333	0.7624	0.6767	0.5831	0.4822	0.3780
stabODEnet ( $\bar{\delta} = 0$ )	0.7775	0.7353	0.6899	0.6418	0.5883	0.5315	0.4713
stabODEnet_d ( $\bar{\delta} = 0$ )	0.6212	0.5968	0.5691	0.5339	0.4973	0.4497	0.3986
shiftODEnet	0.7738	0.7338	0.6926	0.6452	0.5951	0.5430	0.4855

Table 1: MNIST dataset. Comparison of test accuracy across different models as a function of the magnitude  $\eta$  of the FGSM adversarial attack.

$\eta$	0	0.01	0.02	0.03	0.04	0.05	0.06
ODEnet	0.8706	0.7786	0.6523	0.5176	0.3975	0.2937	0.2124
KangODEnet	<b>0.8764</b>	0.7864	0.6584	0.5276	0.4018	0.2979	0.2149
nsdODEnet	0.7039	0.6795	0.6545	0.6312	0.6057	0.5776	0.5482
stabODEnet ( $\bar{\delta} = 2$ )	0.8528	<b>0.7895</b>	0.7066	0.6149	0.5255	0.4452	0.3690
stabODEnet_d ( $\bar{\delta} = 2$ )	0.8474	0.7855	0.7037	0.6132	0.5247	0.4486	0.3713
stabODEnet ( $\bar{\delta} = 1$ )	0.8221	0.7776	<b>0.7239</b>	<b>0.6652</b>	0.6044	0.5501	0.4957
stabODEnet_d ( $\bar{\delta} = 1$ )	0.7929	0.7521	0.7095	0.6637	<b>0.6214</b>	0.5727	0.5212
stabODEnet ( $\bar{\delta} = 0$ )	0.7033	0.6802	0.6583	0.6369	0.6089	<b>0.5823</b>	<b>0.5541</b>
stabODEnet_d ( $\bar{\delta} = 0$ )	0.6751	0.6577	0.6374	0.6160	0.5937	0.5664	0.5411
shiftODEnet	0.6903	0.6691	0.6477	0.6216	0.5982	0.5668	0.5367

Table 2: FashionMNIST dataset. Comparison of test accuracy across different models as a function of the magnitude  $\eta$  of the FGSM adversarial attack.

We observe eventually that the accuracy when the perturbation  $E_*(\varepsilon_*) \in \mathbb{S}_1$  is unstructured is slightly better than that of the case where the perturbation has a diagonal structure, since the diagonal perturbation has a larger Frobenius norm. However, despite this slight loss in accuracy, the diagonal perturbation is computationally cheaper to perform, and hence it may be preferable in some cases.

## 6 Conclusions

We have proposed a method to enhance the stability of a neural ODE by means of a control over the Lipschitz constant of its flow. Enhancing the stability of machine learning models is important since it is desirable that small perturbations in input yield only small changes in output, in particular if perturbations are adversarial attacks.

Since it is known that the Lipschitz constant depends on the logarithmic norm of the Jacobian matrix associated to the neural ODE, we have tuned this parameter at our convenience by suitably perturbing the Jacobian matrix with a perturbation as small as possible in Frobenius norm. We have done so by introducing an optimization problem for which we have proposed a nested two-level algorithm. For a fixed perturbation size, the inner level computes the optimal perturbation with fixed Frobenius norm, while the outer level tunes the perturbation amplitude. We have also proved various properties relevant to both the optimization problem and the algorithm for its solution.

We have embedded the proposed algorithm in the training of the neural ODE to improve its stability. Numerical experiments on the MNIST and FashionMNIST datasets show that an image classifier including a neural ODE in its architecture trained according to our strategy is more stable than the same classifier trained in the classical way, and therefore it is more robust and less vulnerable to adversarial attacks.

## Acknowledgements

N.G. acknowledges that his research was supported by funds from the Italian MUR (Ministero dell'Università e della Ricerca) within the PRIN 2022 Project “Advanced numerical methods for time dependent parametric partial differential equations with applications” and the PRO3 joint project entitled “Calcolo scientifico per le scienze naturali, sociali e applicazioni: sviluppo metodologico e tecnologico”. N.G. and F.T. acknowledge support from MUR-PRO3 grant STANDS and PRIN-PNRR grant FIN4GEO. The authors are members of the INdAM-GNCS (Gruppo Nazionale di Calcolo Scientifico).

## References

- [1] R. T. Q. Chen, Y. Rubanova, J. Bettencourt, and D. K. Duvenaud. Neural Ordinary Differential Equations. In *Advances in Neural Information Processing Systems*, 2018.
- [2] K. He, X. Zhang, S. Ren, and J. Sun. Deep Residual Learning for Image Recognition. In *IEEE Conference on Computer Vision and Pattern Recognition*, 2016.
- [3] E. Celledoni, M. J. Ehrhardt, C. Etmann, R. I. McLachlan, B. Owren, C. B. Schonlieb, and F. Sherry. Structure-preserving deep learning. *European Journal of Applied Mathematics*, 32(5):888–936, 2021.
- [4] B. Biggio, I. Corona, D. Maiorca, B. Nelson, N. Šrndić, P. Laskov, G. Giacinto, and F. Roli. Evasion Attacks against Machine Learning at Test Time. In *Machine Learning and Knowledge Discovery in Databases*, 2013.
- [5] C. Szegedy, W. Zaremba, I. Sutskever, J. Bruna, D. Erhan, I. Goodfellow, and R. Fergus. Intriguing Properties of Neural Networks. In *International Conference on Learning Representations*, 2014.

- [6] I. J. Goodfellow, J. Shlens, and C. Szegedy. Explaining and Harnessing Adversarial Examples. In *International Conference on Learning Representations*, 2015.
- [7] G. Dahlquist and R. Jeltsch. Generalized disks of contractivity for explicit and implicit Runge-Kutta methods. Technical report, CM-P00069451, 1979.
- [8] M. Gottschling, N. V. Antun, A. C. Hansen, and B. Adcock. The troublesome kernel—On hallucinations, no free lunches and the accuracy-stability trade-off in inverse problems. *arXiv preprint arXiv:2001.01258*, 2020.
- [9] E. Haber and L. Ruthotto. Stable architectures for deep neural networks. *Inverse problems*, 34(1):014004, 2017.
- [10] W. Ee. A proposal on machine learning via dynamical systems. *Communications in Mathematics and Statistics*, 1(5):1–11, 2017.
- [11] L. Ruthotto and E. Haber. Deep Neural Networks Motivated by Partial Differential Equations. *Journal of Mathematical Imaging and Vision*, 62(3):352–364, 2020.
- [12] F. Carrara, R. Caldelli, F. Falchi, and G. Amato. On the Robustness to Adversarial Examples of Neural ODE Image Classifiers. In *IEEE International Workshop on Information Forensics and Security*, 2019.
- [13] H. Yan, J. Du, V.Y.F. Tan, and J. Feng. On Robustness of Neural Ordinary Differential Equations. In *International Conference on Learning Representations*, 2020.
- [14] M. Li, L. He, and Z. Lin. Implicit Euler Skip Connections: Enhancing Adversarial Robustness via Numerical Stability. In *International Conference on Machine Learning*, 2020.
- [15] F. Carrara, R. Caldelli, F. Falchi, and G. Amato. Defending Neural ODE Image Classifiers from Adversarial Attacks with Tolerance Randomization. In *International Conference on Pattern Recognition*, 2021.
- [16] F. Carrara, R. Caldelli, F. Falchi, and G. Amato. Improving the Adversarial Robustness of Neural ODE Image Classifiers by Tuning the Tolerance Parameter. *Information*, 13(12):555, 2022.
- [17] R. Caldelli, F. Carrara, and F. Falchi. Tuning Neural ODE Networks to Increase Adversarial Robustness in Image Forensics. In *IEEE International Conference on Image Processing*, 2022.
- [18] Q. Kang, Y. Song, Q. Ding, and W.P. Tay. Stable Neural ODE with Lyapunov-Stable Equilibrium Points for Defending against Adversarial Attacks. In *Advances in Neural Information Processing Systems*, 2021.
- [19] X. Li, Z. Xin, and W. Liu. Defending Against Adversarial Attacks via Neural Dynamic System. In *Advances in Neural Information Processing Systems*, 2022.
- [20] Y. Huang, Y. Yu, H. Zhang, Y. Ma, and Y. Yao. Adversarial Robustness of Stabilized Neural ODE Might Be From Obfuscated Gradients. In *Mathematical and Scientific Machine Learning*, 2022.
- [21] W. Cui, H. Zhang, H. Chu, P. Hu, and Y. Li. On robustness of neural ODEs image classifiers. *Information Sciences*, 632:576–593, 2023.

- [22] V. Purohit. Ortho-ODE: Enhancing Robustness of Neural ODEs against Adversarial Attacks. *arXiv preprint arXiv:2305.09179*, 2023.
- [23] E. Celledoni, D. Murari, B. Owren, C.-B. Schönlieb, and F. Sherry. Dynamical Systems-Based Neural Networks. *SIAM Journal on Scientific Computing*, 45(6):A3071–A3094, 2023.
- [24] F. Sherry, E. Celledoni, M. J. Ehrhardt, D. Murari, B. Owren, and C.-B. Schönlieb. Designing stable neural networks using convex analysis and ODEs. *Physica D: Nonlinear Phenomena*, 463:134–159, 2024.
- [25] N. Guglielmi and C. Lubich. Matrix Stabilization Using Differential Equations. *SIAM Journal on Numerical Analysis*, 55(6):3097–3119, 2017.
- [26] N. Guglielmi, C. Lubich, and S. Sicilia. Rank-1 Matrix Differential Equations for Structured Eigenvalue Optimization. *SIAM Journal on Numerical Analysis*, 61(4):1737–1762, 2023.
- [27] N. Guglielmi, A. De Marinis, A. Savostianov, and F. Tudisco. Contractivity of neural ODEs: an eigenvalue optimization problem. *arXiv preprint arXiv:2402.13092*, 2024.
- [28] N. Guglielmi and S. Sicilia. Stabilization of a matrix via a low-rank-adaptive ODE. *BIT Numerical Mathematics*, 64(4):38, 2024.
- [29] L. Deng. The MNIST database of handwritten digit images for machine learning research. *IEEE Signal Processing Magazine*, 29(6):141–142, 2012.
- [30] H. Xiao, K. Rasul, and R. Vollgraf. Fashion-MNIST: a novel image dataset for benchmarking machine learning algorithms. *arXiv preprint arXiv:1708.07747*, 2017.
- [31] T. Kato. *Perturbation Theory for Linear Operators*. Springer, 2013.
- [32] N. Guglielmi and S. Sicilia. A low-rank ODE for spectral clustering stability. *Linear Algebra and its Applications*, 2024.
- [33] J.E. Avron and B. Simon. Analytic Properties of Band Functions. *Annals of Physics*, 110(1):85–101, 1978.